



Contents lists available at ScienceDirect

Aeolian Research

journal homepage: www.elsevier.com/locate/aeolia

The developmental trend and influencing factors of aeolian desertification in the Zoige Basin, eastern Qinghai–Tibet Plateau

Guangyin Hu*, Zhibao Dong, Junfeng Lu, Changzhen Yan

Key Laboratory of Desert and Desertification, Cold and Arid Regions Environmental and Engineering Research Institute, Chinese Academy of Sciences, Lanzhou 730000, China

ARTICLE INFO

Article history:
Available online xxx

Keywords:
Aeolian desertification
Remote sensing
Zoige Basin
Qinghai–Tibet Plateau

ABSTRACT

The Zoige Basin is located in the northeastern region of the Qinghai–Tibet Plateau and covers an area of 19,400 km². At a mean altitude of 3500 m, the basin is highly sensitive to global environmental change and human disturbance due to its high elevation and fragile cold environment. The process of aeolian desertification in the basin can be clearly recognized in Landsat images that show the development of sand sheets and dunes over time. To monitor the spatial and temporal changes of aeolian desertification in the Zoige Basin, we analyzed Landsat images recorded in 1975, 1990, 2000, 2005, and 2010. Results showed that aeolian desertification increased rapidly from 1975 to 1990, was stable from 1990 to 2000, decreased slightly from 2000 to 2005, and decreased sharply from 2005 to 2010. Increasing temperature, overgrazing, rodent damage, and drainage of wetlands were considered the key driving factors of the expansion of aeolian desertification. A number of political measures were initiated in the 1990s to slow desertification, but the countermeasures of grazing prohibition, enclosures, and paving straw checkerboard barriers were not implemented until around 2005. These measures resulted in a dramatic recovery of aeolian desertified land between 2005 and 2010. Based on the cause analysis, anthropogenic factors were identified as the dominant driving force for both development and recovery of aeolian desertified land.

© 2015 Elsevier B.V. All rights reserved.

1. Introduction

The Zoige Basin is recognized as a “natural reservoir” for the Yellow River as nearly 30% of the Yellow River's total flow originates from the basin's wetland. In addition to having the most extensive distribution of high-altitude peat bogs in the world, this area has a large area of high-quality grasslands, serving as the fifth largest livestock base in China. However, recent investigations have revealed that aeolian desertification has become one of the most severe environmental problems, threatening the important ecological roles of this region. Moreover, as a result of climate change and artificial drainage, the total wetland area of this basin has shrunk rapidly since the 1980s (Pang et al., 2010) and the water table in the Zoige peat-wetlands has severely declined (Xiang et al., 2009). With the lowering of the water table, the decomposition of the peat deposits and the accelerated carbon emissions from peat respiration have become a potential ecosystem crisis (Guo et al., 2013) despite the fact that human–social

factors cause most of the natural CO₂ emissions in the Zoige wetlands (Cui et al., 2014).

Aeolian desertification occurring on the high-altitude Qinghai–Tibet Plateau has received attention only recently (Shen et al., 2012; Zhang et al., 2012). In the 1990s, caesium-137 (¹³⁷Cs) was used to study wind erosion in this area (Yan et al., 2001), and in the mid 2000s, the influence of desertification on vegetation pattern variations was investigated in the cold semi-arid grasslands of the plateau (Li et al., 2006). The majority of the Qinghai–Tibet Plateau lies at altitudes higher than 3000 m above sea level, so this region has a cold high-altitude climate. However, the mean annual temperature for the entire plateau area has increased significantly since the 1960s, and particularly since the 1980s. The annual increased rate in temperature of 0.25 °C per decade is primarily influenced by warming in winter and autumn (0.40 °C and 0.26 °C per decade, respectively) (You et al., 2010). The rapid climate change in this region is causing various environmental problems, including glacier retreat (Lei et al., 2013; Wang et al., 2013), permafrost degradation (Jin et al., 2008; Yang et al., 2010), grassland degradation (Wang et al., 2011, 2008; Zeng et al., 2013), and aeolian desertification (Hu et al., 2012; Xue et al., 2009).

Because of its important roles in water conservation, biodiversity protection, and wetland conservation, the Zoige Wetland National

* Corresponding author at: Cold and Arid Regions Environmental and Engineering Research Institute, Chinese Academy of Sciences, No. 320, West Donggang Road, Lanzhou, Gansu Province 730000, China. Tel.: +86 (0)931 496 7496.

E-mail address: Guangyinhu0830@163.com (G. Hu).

Natural Reserve was established by the Chinese government in 1994 to protect the marsh and the surrounding areas. The source regions of the Yangtze, Yellow, and Lancang Rivers were classified as provincial nature reserves in 2000 and were upgraded to national nature reserves in 2003. Since 2000, Chinese government has invested nearly RMB 20 billion (approximately US \$3.33 billion) to control the serious environmental problems in this region, including aeolian desertification. The important eco-environmental and socio-economic roles of this region highlight the urgent need to study the evolution of aeolian desertification in order to understand its driving forces. This is the goal of the present study.

2. Study area

The Zoige Basin is located in the eastern part of the Qinghai–Tibet Plateau where China's Gansu province, Sichuan province, and Qinghai province meet (Fig. 1). It lies between latitudes 32°17'N and 32°7'N and longitudes 101°30'E and 103°22'E, covering an area of 19,400 km². At a mean altitude of 3500 m, the basin is surrounded by the Anymaqen Mountains to the northwest, the Minshan Mountains to the east, and the Qionglai Mountains to the south. This region includes three counties (Maqu county of Gansu province, Zoige county, and Hongyuan county of Sichuan province). The Zoige Basin is characterized by wide meandering river valleys and lakes dotted among low hills. Deep Quaternary deposits have accumulated throughout the basin. The main rivers in the basin include the Yellow River and its tributaries, including the White River, the Black River, and the Jiaqu River.

The Zoige Basin has a humid, frigid, continental monsoon climate due to its high altitude and is characterized by a long winter and a relatively short summer. The mean annual precipitation ranges from 654 to 780 mm, and the mean annual potential evaporation ranges from 1110 to 1273 mm. The mean annual temperature ranges from 0.7 to 3.3 °C, and as a result of this low air temperature, vegetation gross primary productivity is very low. The vegetation in this region is dominated by subalpine meadow and marsh vegetation. Deep loose deposits combined with the cold and wet climate provide favorable conditions for the development of marshes and peat. The soil mainly includes alpine peat soils, alpine meadow soils, and subalpine meadow soils. Carbonate meadow soils, salt-affected meadow soils, and aeolian sandy soils have developed in some locations due to land degradation (Huo et al., 2013).

3. Materials and methods

3.1. Data sources

The development of sand sheets and dunes that can be clearly recognized in remote-sensing images indicates the presence of aeolian desertification (Liu, 1996). To assess the evolution of desertification in the study area, remote sensing and geographical information system (GIS) software were employed to monitor the extent of aeolian desertification five times over 35 years (in 1975, 1990, 2000, 2005, and 2010). The data sources included Landsat multi-spectral scanner (MSS) images acquired in 1975, with an 80-m spatial resolution; Landsat Thematic Mapper (TM) images acquired in 1990 and 2005, with a 30-m spatial resolution; and Landsat Enhanced Thematic Mapper (ETM+) images acquired in 2000 and 2010, with a 30-m resolution. Images recorded between June and October were selected for analysis because desertified lands are more easily recognized during this period when vegetation growth is at its maximum. Thematic maps, including land use and geomorphologic maps, were used as supplementary data sources.

3.2. Image processing and interpretation

Image processing included georeferencing the images, mapping the satellite data, and data processing as well as field validation. The TM images from 2005 were georeferenced using the Image Analyst function of version 7.01 of the Modular GIS Environment (MGE) software (Intergraph, Madison, AL, USA). Georeferencing was based on more than 40 ground control points (GCPs) derived from relief maps of the study area at a scale of 1:100,000 created in 1980 by the Chinese State Bureau of Surveying and Mapping. The MSS images from 1975, the TM images from 1990, and the ETM+ images from 2000 and 2010 were matched with the georeferenced 2005 TM images. During image georeferencing and matching, 30 to 40 GCPs were selected in each image and the root-mean-square error of the geometrical rectification between the two images was limited to 1 or 2 pixels in flat land and 2 or 3 pixels in mountainous regions; results fell within the range of resolutions considered appropriate for large-area surveys. A second-order transformation based on the nearest-neighbor method was used to resample the images to produce 30 × 30 m pixels for the TM and ETM+ images and 80 × 80 m pixels for the MSS images. We

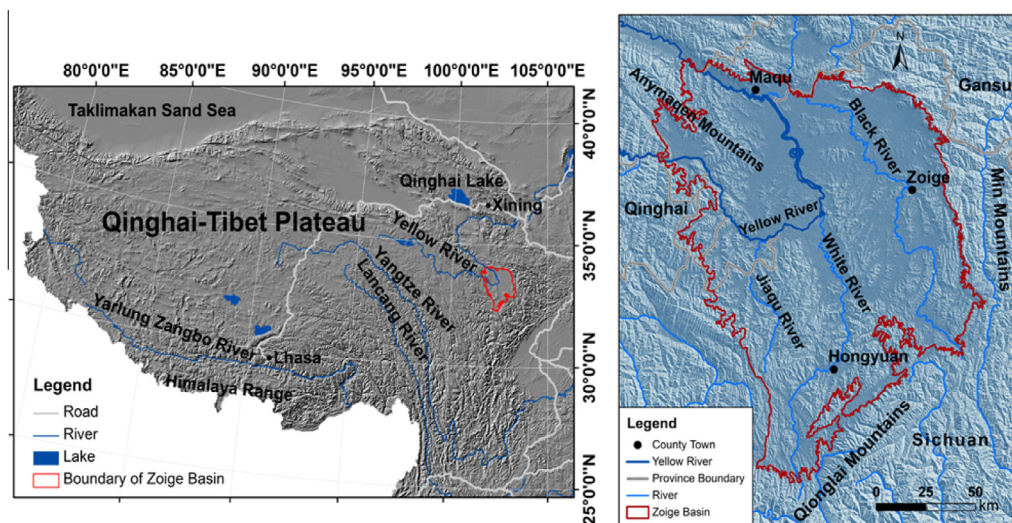


Fig. 1. Location of the Zoige Basin.

assumed that this resolution would be adequate for our purpose since broad coverage of a large landscape was more important than precise mapping of fine details.

Wavelength bands 4, 3, and 2 of the TM images were combined to generate false-color images that bore richer information and less redundancy. Databases of aeolian desertification in the study area in each of the five monitored years were derived from the composite false-color images by means of a visually interactive interpretation method, with classification assisted by the MGE software. The mapping accuracy of this method was considered to be higher than that of image classification using only the algorithms provided by the image processing software. The minimum map patch size was 6×6 pixels, which was equivalent to 180×180 m on the ground. The positioning error was one pixel on the screen, which was equivalent to 30 m on the ground in the TM and ETM+ images and 80 m on the ground in the MSS images.

The images were interpreted by three doctoral students who majored in geography. The interpretation results for images in a sampled area were validated in the field. Subsequent corrections were made after field validation to provide classification accuracy greater than 95%.

3.3. Classification system for aeolian desertification

In the Zoige Basin, the depositional features are mainly dunes and sand sheets (Fig. 2). Based on the classification of aeolian desertification in the arid and semi-arid regions in northern China (Wang, 2004), the extent of aeolian desertification was graded as slight, moderate, or severe, depending on the landscape indicators listed in Table 1.

4. Results and Discussion

4.1. Development of desertification

The five aeolian desertification maps produced from the Landsat images clearly showed that the degree of aeolian desertification varied over the 35 years from 1975 to 2010 (Fig. 3). The

Table 1

Landscape indicators that could be easily identified in the remote sensing images.

Degree of aeolian desertification	Landscape indicators
Slight	Fixed dunes (sandy land), areas of semi-exposed gravel
Moderate	Semi-fixed dunes (sandy land), areas of bare gravel
Severe	Shifting dunes (sandy land)

development of aeolian desertification can be divided into three phases: increasing (1975–1990), stable (1990–2005), and decreasing (2005–2010). From 1975 to 1990, the total area of aeolian desertification increased by 2147 km^2 at a rate of 143 km^2 per year, while from 2005 to 2010 the total area decreased by 2587 km^2 at a rate of 517 km^2 per year. Between 1990 and 2000, however, the total area of aeolian desertification increased by only 26 km^2 , and from 2000 to 2005 it decreased by 67 km^2 . Over the entire study period from 1975 to 2010, the total area of desertification decreased by 482 km^2 (the areas of slight, moderate, and severe desertification decreased by 31, 415, and 36 km^2 , respectively). It was also clear from the maps that the change in the total area of desertified land resulted mainly from the changes to areas affected by light and moderate desertification; the area of severe desertification remained stable at a low level, varying between 152 km^2 in 2000 and 99 km^2 in 2010 (Fig. 3). This suggests that the Zoige Basin had substantial recovery of aeolian desertified land.

4.2. Distribution of desertification

Fig. 4 shows the spatial distribution of aeolian desertification in the study area in 1975, 1990, 2000, 2005 and 2010. The area of aeolian desertified land was the most widely distributed in 2000. At 3211 km^2 it accounted for 16.6% of the total land area in the Zoige Basin. Areas of slight, moderate, and severe aeolian desertification were 1473 km^2 (45.9%), 1586 km^2 (49.4%), and 152 km^2 (4.7%), respectively, of the total area of aeolian desertified land. However, the area of aeolian desertification shrank to 557 km^2 in 2010,

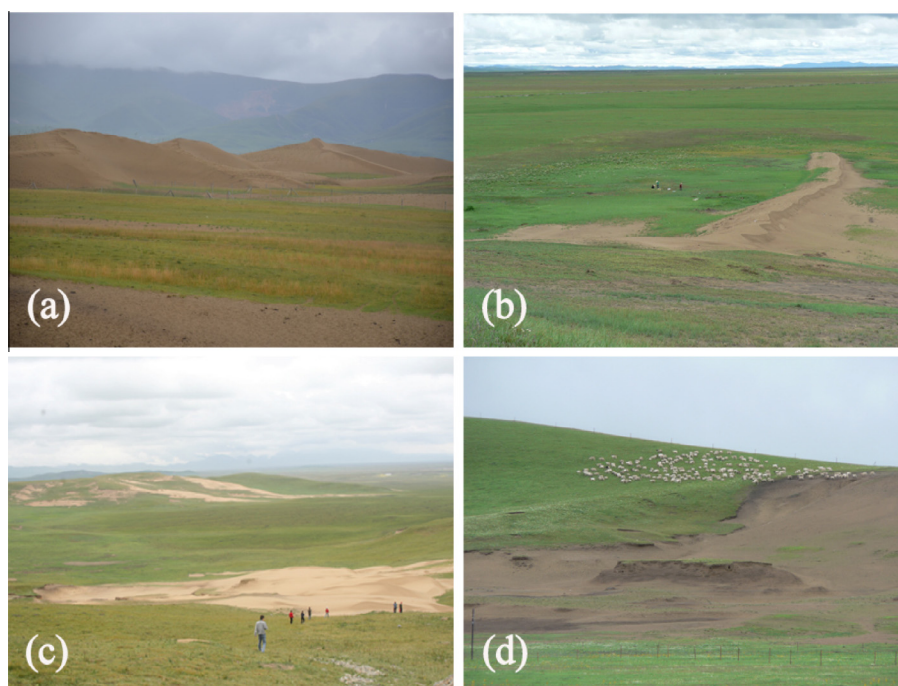


Fig. 2. Typical landscape of aeolian desertification in the Zoige Basin: (a) shifting dunes, (b and c) shifting sandy land, (d) bare land.

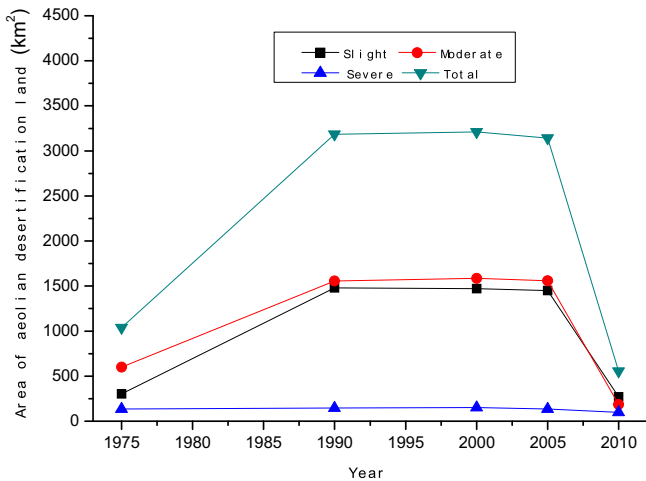


Fig. 3. The extent of aeolian desertification in 1975, 1990, 2000, 2005, and 2010.

accounting for only 2.9% of the total land area in the Zoige Basin (Fig. 4).

Abundant sandy material is one of the preconditions for aeolian desertification. Geologically, the Zoige Basin is a stable massif that experienced planation during the Tertiary and relatively slower uplift than the rest of the Qinghai–Tibetan Plateau during the

Quaternary, when deep deposits accumulated throughout the basin and resulted in the formation of a block basin.

4.3. Climatic factors

Changes in the mean annual climate in the study area were analyzed based on meteorological data recorded by the Maqu and Zoige meteorological stations from 1975 to 2010. The monthly climatic data were also analyzed based on data recorded from 2004 to 2010 at these two stations.

From 1975 to 2010, the mean annual wind speed decreased at a mean rate of 0.01 and 0.10 m s⁻¹ per decade at the Maqu and Zoige stations, respectively (Fig. 5). Since increased wind speed is required to cause increased desertification, these data indicate that wind speed was not the principal factor responsible for the development of aeolian desertification in this region.

The climate in the Zoige Basin tended to become warmer and drier between 1975 and 2010 (Fig. 6), with the mean annual precipitation decreasing at an average rate of 17.19 mm per decade. Decreased precipitation would have affected vegetation growth and soil moisture retention, thereby increasing aeolian desertification. The mean annual temperature increased at an average rate of 0.52 °C per decade, and this increase accelerated during the last 10 years of the study period to a rate of 1.02 °C per decade (Fig. 6). Both values are much greater than the mean global rate of increase (0.03–0.06 °C per decade).

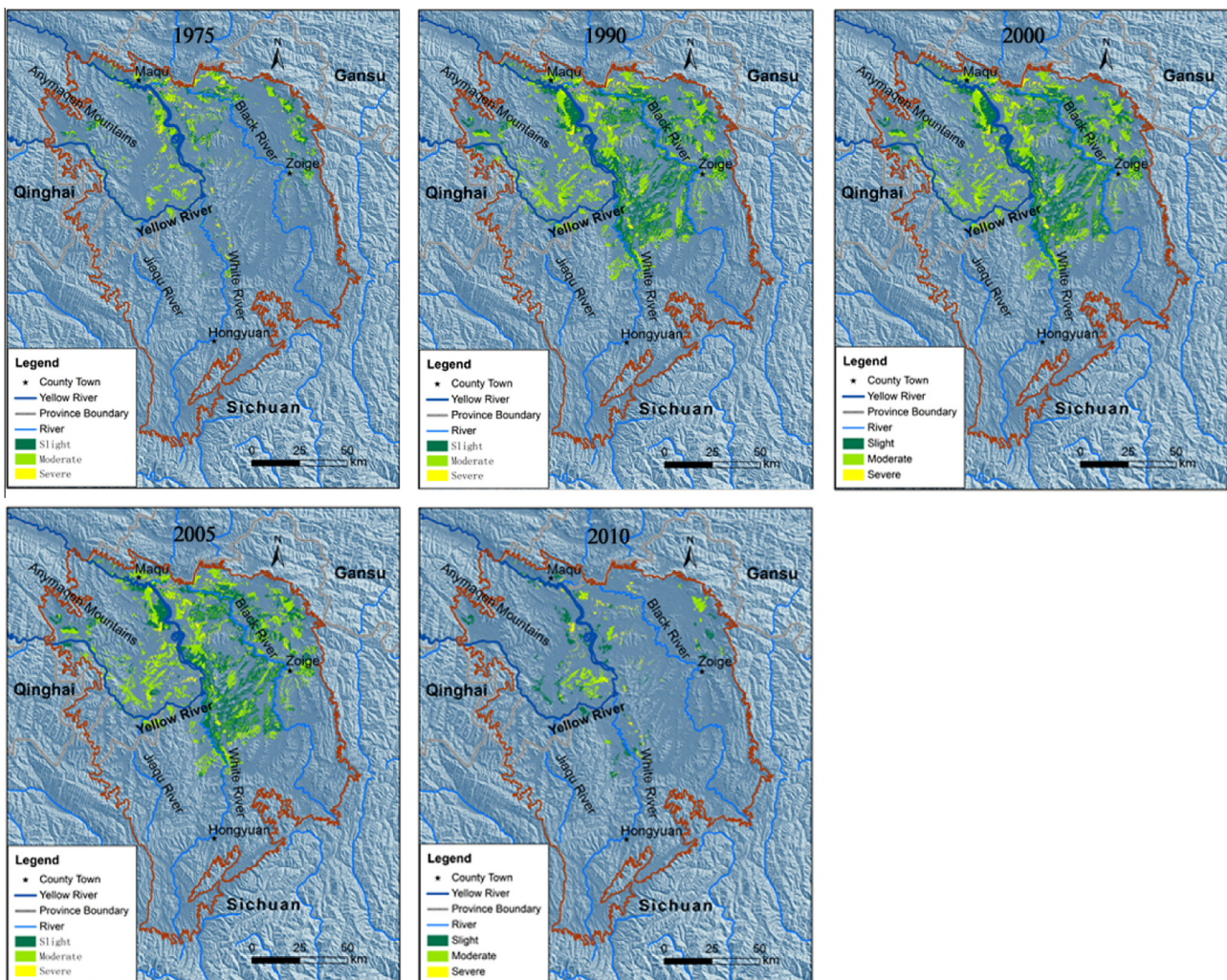


Fig. 4. Distribution of aeolian desertification in the Zoige Basin in 1975, 1990, 2000, 2005, and 2010.

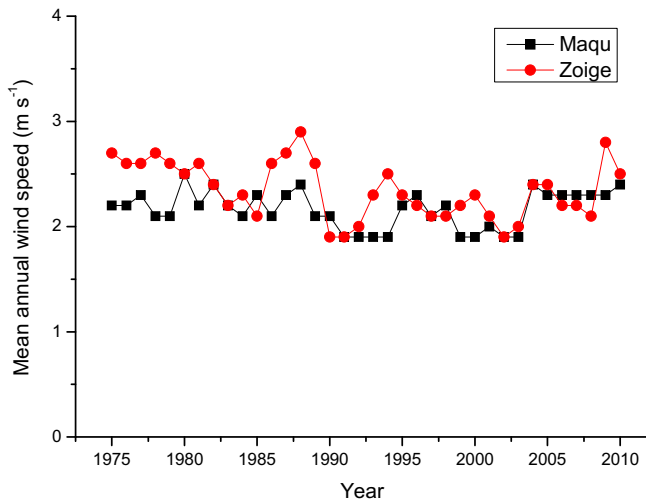


Fig. 5. Changes in the mean annual wind speed between 1975 and 2010 in the Zoige Basin.

Against this background of a long-term annual temperature increase, seasonal variations in climate (Fig. 7) also aggravated the severity of aeolian desertification in the Zoige Basin. The monthly precipitation is mainly concentrated between May and October, accounting for 89.2% of the annual total (610 mm). During the 6 months from October to April, the mean monthly temperature remains below 0 °C, and from December to February, the mean monthly temperature generally decreases to below –5 °C. This dry cold climate leads most vegetation stops growing or dies. As a result, vegetation cover decreases and the land becomes vulnerable to wind erosion, although as the soil dries out, it becomes less resistant to wind erosion. During the spring, the number of days with a strong wind (i.e., with maximum wind speed $\geq 17 \text{ m s}^{-1}$) reaches its maximum. Although strong winds only occur on average 18 days per year, a sand-blowing wind (i.e., average 10-min wind speed $\geq 6 \text{ m s}^{-1}$) can occur up to 276 days per year. The combination of a dry, cold, and windy climate with periods of low vegetation cover promotes wind erosion and leads to various aeolian desertification landscape forms, such as sandy land and sand dunes.

4.4. Anthropogenic factors

A previous study documented that anthropogenic factors, such as overgrazing and water system drainage, play an important role in aeolian desertification in the Zoige Basin (Dong et al., 2010). Although natural factors, such as climatic variations, provide the background for its development, the range in climatic variations does not appear to have exceeded the threshold required for aeolian desertification to develop. Human disturbances appear to be the most important factors responsible for aeolian desertification in the Zoige Basin. Evidence for this is our observation that degraded meadows could naturally recover once they had been fenced to protect them from grazing animals.

The statistical data from Maqu and Zoige county annuals indicate that the total population in the Zoige Basin increased from 72,000 to 130,000 from 1978 to 2010, with a net increase of 57,900 (80.4% of the 1978 population) (Fig. 8). At the same time, the number of livestock in the basin increased correspondingly from 1.53 million in 1978 to 2.15 million in 2010, giving a net increase of 0.62 million (40.5% of the 1978 livestock number).

Human disturbances leading to aeolian desertification in the Zoige Basin mainly include overgrazing, drainage of water systems, land reclamation for agriculture, unsustainable collection of medicinal herbs and peat, and mining. However, compared with overgrazing and drainage of water systems, the other factors were only significant in some local areas. Since the 1990s, specific political countermeasures have been carried out to combat aeolian desertification; however, the countermeasures of grazing prohibition, enclosures, and paving straw checkerboard barriers were not implemented until around 2005, which resulted in a dramatic recovery of aeolian desertified land from 2005 to 2010.

As the “tragedy of the commons” led to the problem of overgrazing in common pasture areas throughout the study area in the 1970s and 1980s, it was necessary to adjust the grazing rights of local people to prevent further overgrazing (Allsopp et al., 2007). Since the 1990s, the government has rented grassland to herdsman-households who could make their own management decisions. In Maqu county, for example, the local government has invested RMB 65.15 million in environmental protection, including renting 8300 km² of grassland, enclosing 1650 km² of grassland, planting 133 km² of artificial grassland, and recovering 2400 km² of rodent-damaged grassland.

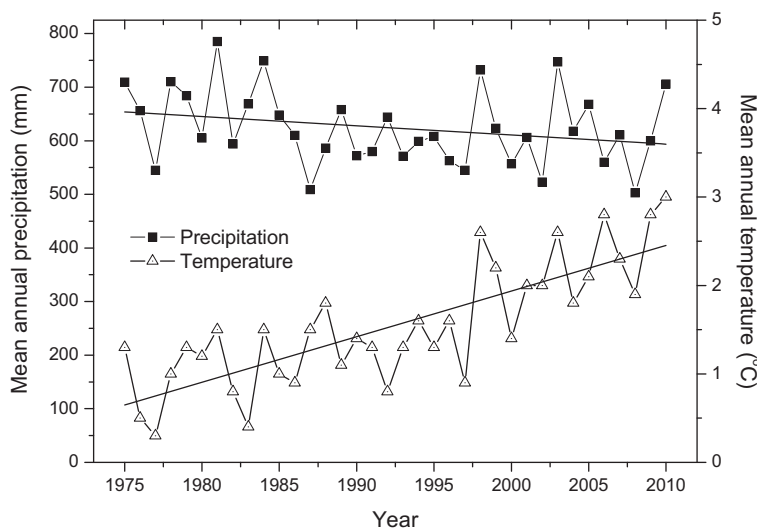


Fig. 6. Changes in the mean annual temperature and precipitation between 1975 and 2010 in the Zoige Basin. (The meteorological data represent the average value of the Zoige and Maqu stations.)

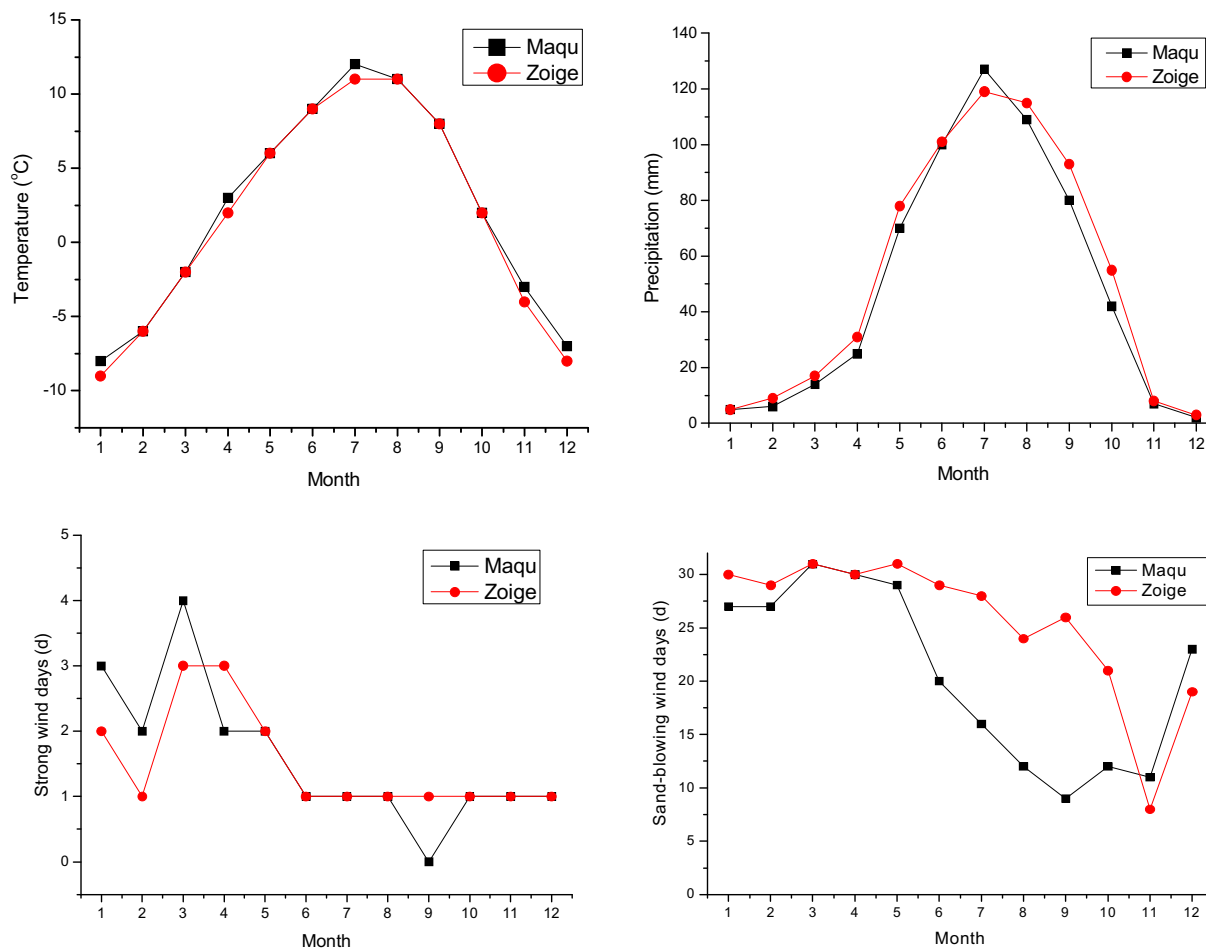


Fig. 7. Seasonal variations in climate. Strong wind days represent days with a maximum wind speed $\geq 17 \text{ m s}^{-1}$; days with sand-blowing wind have an average 10-min wind speed $\geq 6 \text{ m s}^{-1}$. Values represent the long-term mean from 2004 to 2010 at the Zoige and Maqu meteorological stations.

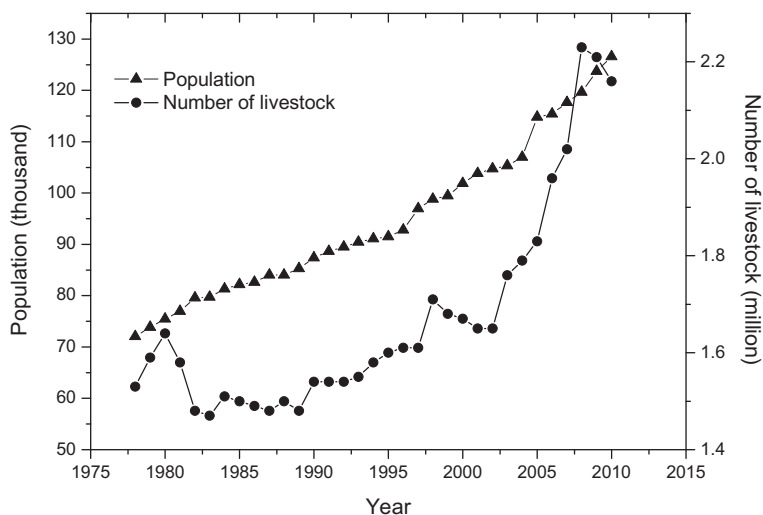


Fig. 8. The increase in population and livestock in the Zoige Basin from 1978 to 2010.

Furthermore, to protect the main water supply area of the Yellow River, the Chinese government has arranged a long-term eco-environmental protection project that is divided into two phases. Phase 1, from 2007 to 2010, mainly focused on the protection and recovery of grasslands and wetlands and included actions such

as stopping artificial drainage and building dams to preserve water. Phase 2, from 2010 to 2020, mainly focuses on water conservation and water supply areas and is taking comprehensive countermeasures to fully recover the eco-environmental functions of this region.

5. Conclusions

Remote sensing mapping showed that aeolian desertification increased in severity between 1975 and 1990, with the area of desertified land expanding rapidly. By 1990, aeolian desertified land had spread by 2147 km², an increase of 207% over the total area in 1975 at an increased rate of 143 km² per year. However, from 2005 to 2010, the area of desertified land decreased by 2587 km² at a rate of 518 km² per year.

The climate in the Zoige Basin became warmer and drier between 1975 and 2010. This combined with anthropogenic factors, such as overgrazing and drainage of water systems, and a dry, cold, and windy climate during the winter and spring when vegetation cover is low promoted wind erosion and led to various aeolian desertification landscape forms. Following the implementation of specific countermeasures in 2005, the area of aeolian desertified land recovered dramatically. Although aeolian desertification in the Zoige Basin has received increasing attention in recent years, the historical movement of the aeolian sandy sediments is still poorly understood. In future research, we intend to collect profile samples in order to gain a detailed chronology for understanding the timing of aeolian processes and associated environmental conditions in this region.

Acknowledgments

We are grateful for the financial support provided by the National Natural Science Foundation of China (Grant No. 41201002), the Ministry of Science and Technology of the People's Republic of China (2013CB956000), the China Postdoctoral Science Foundation funded project (Grant No. 2012M512050), and the Opening Fund of the Key Laboratory for Desert and Desertification in Cold and Arid Regions, Chinese Academy of Sciences (KLDD-2014-009).

References

- Allsopp, N., Laurent, C., Debeaudoin, L.M.C., Igshaan Samuels, M., 2007. Environmental perceptions and practices of livestock keepers on the Namaqualand commons challenge conventional rangeland management. *J. Arid Environ.* 70, 740–754.
- Cui, Q., Wang, X., Li, C., Cai, Y., Liu, Q., Li, R., 2014. Ecosystem service value analysis of CO₂ management based on land use change of Zoige alpine peat wetland Tibetan Plateau. *Ecol. Eng.*
- Dong, Z., Hu, G., Yan, C., Wang, W., Lu, J., 2010. Aeolian desertification and its causes in the Zoige Plateau of China's Qinghai–Tibetan Plateau. *Environ. Earth Sci.* 59, 1731–1740.

- Guo, X., Du, W., Wang, X., Yang, Z., 2013. Degradation and structure change of humic acids corresponding to water decline in Zoige peatland, Qinghai–Tibet Plateau. *Sci. Total Environ.* 445–446, 231–236.
- Hu, G., Dong, Z., Lu, J., Yan, C., 2012. Driving forces responsible for aeolian desertification in the source region of the Yangtze River from 1975 to 2005. *Environ. Earth Sci.* 66, 257–263.
- Huo, L., Chen, Z., Zou, Y., Lu, X., Guo, J., Tang, X., 2013. Effect of Zoige alpine wetland degradation on the density and fractions of soil organic carbon. *Ecol. Eng.* 51, 287–295.
- Jin, H., Yu, Q., Wang, S., Lü, L., 2008. Changes in permafrost environments along the Qinghai–Tibet engineering corridor induced by anthropogenic activities and climate warming. *Cold Reg. Sci. Technol.* 53, 317–333.
- Lei, Y., Yao, T., Bird, B.W., Yang, K., Zhai, J., Sheng, Y., 2013. Coherent lake growth on the central Tibetan Plateau since the 1970s: characterization and attribution. *J. Hydrol.* 483, 61–67.
- Li, X.R., Jia, X.H., Dong, G.R., 2006. Influence of desertification on vegetation pattern variations in the cold semi-arid grasslands of Qinghai–Tibet Plateau, Northwest China. *J. Arid Environ.* 64, 505–522.
- Liu, J.Y., 1996. Macro-scale Survey and Dynamic Study of Natural Resources and Environment of China by Remote Sensing. China Science and Technology Press, Beijing.
- Pang, A., Li, C., Wang, X., Hu, J., 2010. Land use/cover change in response to driving forces of Zoige county, China. *Procedia Environ. Sci.* 2, 1074–1082.
- Shen, W., Li, H., Sun, M., Jiang, J., 2012. Dynamics of aeolian sandy land in the Yarlung Zangbo River basin of Tibet, China from 1975–2008. *Global Planet. Change* 86–87, 37–44.
- Wang, G., Bai, W., Li, N., Hu, H., 2011. Climate changes and its impact on tundra ecosystem in Qinghai–Tibet Plateau, China. *Climatic Change* 106, 463–482.
- Wang, G., Li, Y., Wang, Y., Wu, Q., 2008. Effects of permafrost thawing on vegetation and soil carbon pool losses on the Qinghai–Tibet Plateau, China. *Geoderma* 143, 143–152.
- Wang, T., 2004. Study on sandy desertification in China: 3. Key regions for studying and combating sandy desertification. *J. Desert Res.* 24, 1–9.
- Wang, X., Siegert, F., Zhou, A.-G., Franke, J., 2013. Glacier and glacial lake changes and their relationship in the context of climate change, Central Tibetan Plateau 1972–2010. *Global Planet. Change* 111, 246–257.
- Xiang, S., Guo, R., Wu, N., Sun, S., 2009. Current status and future prospects of Zoige Marsh in Eastern Qinghai–Tibet Plateau. *Ecol. Eng.* 35, 553–562.
- Xue, X., Guo, J., Han, B., Sun, Q., Liu, L., 2009. The effect of climate warming and permafrost thaw on desertification in the Qinghai–Tibetan Plateau. *Geomorphology* 108, 182–190.
- Yan, P., Dong, Z., Dong, G., Zhang, X., Zhang, Y., 2001. Preliminary results of using¹³⁷Cs to study wind erosion in the Qinghai–Tibet Plateau. *J. Arid Environ.* 47, 443–452.
- Yang, M., Nelson, F.E., Shiklomanov, N.I., Guo, D., Wan, G., 2010. Permafrost degradation and its environmental effects on the Tibetan Plateau: a review of recent research. *Earth Sci. Rev.* 103, 31–44.
- You, Q., Kang, S., Pepin, N., Flügel, W.-A., Sanchez-Lorenzo, A., Yan, Y., Zhang, Y., 2010. Climate warming and associated changes in atmospheric circulation in the eastern and central Tibetan Plateau from a homogenized dataset. *Global Planet. Change* 72, 11–24.
- Zeng, C., Zhang, F., Wang, Q., Chen, Y., Joswiak, D.R., 2013. Impact of alpine meadow degradation on soil hydraulic properties over the Qinghai–Tibetan Plateau. *J. Hydrol.* 478, 148–156.
- Zhang, K., Qu, J., Han, Q., An, Z., 2012. Wind energy environments and aeolian sand characteristics along the Qinghai–Tibet Railway, China. *Sed. Geol.* 273–274, 91–96.